A b i n i t i o study of the energetics of the spinallowed and spinforbidden decomposition of HN3

Millard H. Alexander, HansJoachim Werner, Terrence Hemmer, and Peter J. Knowles

Citation: The Journal of Chemical Physics **93**, 3307 (1990); doi: 10.1063/1.458811
View online: http://dx.doi.org/10.1063/1.458811
View Table of Contents: http://scitation.aip.org/content/aip/journal/jcp/93/5?ver=pdfcov
Published by the AIP Publishing

Ab initio study of the energetics of the spin-allowed and spin-forbidden decomposition of HN_3

Millard H. Alexander[a] and Hans-Joachim Werner
Fakultät für Chemie der Universität Bielefeld, 4800 Bielefeld 1, Federal Republic of Germany

Terrence Hemmer
Department of Chemistry, University of Maryland, College Park, Maryland 20742

Peter J. Knowles
School of Chemical and Molecular Sciences, University of Sussex, Falmer Brighton BN1 9QJ, United Kingdom

(Received 30 March 1990; accepted 7 May 1990)

We describe an investigation of the energetics of the dissociation of ground state hydrazoic acid HN_3. The study is limited to the lowest energy spin-allowed and spin-forbidden decomposition pathways, namely $HN_3(\tilde{X}\,^1A') \rightarrow N_2(X\,^1\Sigma_g^+) + NH(a\,^1\Delta, X\,^3\Sigma^-)$ and $HN_3(\tilde{X}\,^1A') \rightarrow N_3(\tilde{X}\,^2\Pi_g) + H(^2S)$. Complete active space SCF and multireference configuration interaction calculations with large basis sets are used (a) to determine the NNN–H and NN–NH bond dissociation energies of HN_3, (b) to locate the geometry of the transition state for the spin-forbidden decomposition and the corresponding activation energy, and (c) to investigate the magnitude and origin of the exit channel barrier in the spin-allowed decomposition channel.

I. INTRODUCTION

In many photodissociation reactions one or more of the diatomic fragments are formed in open-shell electronic states.[1–3] The distribution of the products among the various possible electronic and/or fine-structure levels can, in principle, provide considerable insight into the photolytic mechanism. From a theoretical point of view the mechanism of ground state decomposition is easier to characterize, since it is easier to determine accurate *ab initio* descriptions of ground state potential energy surfaces. Ground state decomposition can be probed most selectively by overtone pumping.[4–6] Particularly noteworthy have been the work of Crim, Rizzo, and co-workers on the decomposition of hydrogen peroxide[7,8] and that of Stephenson, Casassa, Foy, and King on the decomposition of HN_3.[4–6]

In an earlier paper[9] we investigated the origin of preferential population of spin levels in the NH products formed in the spin-forbidden decomposition of HN_3:

$$HN_3(\tilde{X}\,^1A') \rightarrow N_2(X\,^1\Sigma_g^+) + NH(X\,^3\Sigma^-), \qquad (1)$$

as well as the preferential population of Λ-doublet levels in the $NH(a\,^1\Delta)$ products formed in the spin-allowed process

$$HN_3(\tilde{X}\,^1A') \rightarrow N_2(X\,^1\Sigma_g^+) + NH(a\,^1\Delta). \qquad (2)$$

Decomposition according to Eq. (1) occurs by a spin–orbit induced crossing between the singlet surface, which correlates asymptotically to $N_2(X\,^1\Sigma_g^+) + NH(a\,^1\Delta)$, and the lowest triplet surface. As illustrated schematically in Fig. 1, the triplet asymptote lies below the singlet asymptote by 12 664 cm^{-1}, which is the splitting between the $X\,^3\Sigma^-$ and $a\,^1\Delta$ states of NH.[10] In the molecular region the triplet surface correlates with an electronically excited triplet state of HN_3. Although our primary aim in this previous paper[9] was the understanding of the nonstatistical fine-structure populations seen in both overtone[4–6] and IRMPD[11] experiments, we were also able to determine a rough estimate of the height of the barrier for the spin-forbidden decomposition. This theoretical estimate ($E_a = 12\,300$ cm^{-1}), to which zero point corrections were not added, agreed well with the value $E_a \cong 150 kJ/mol = 12\,700$ cm^{-1} estimated by Kajimoto *et al.*[12] from thermal dissociation studies in a shock tube, although other shock tube studies[13,14] have yielded considerably different activation energies.

The height of the barrier to the spin-forbidden decomposition of HN_3 and the topology of the singlet and triplet potential energy surfaces in the neighborhood of this barrier will influence the rate at which products are formed and the degree of rotational and vibrational excitation of these products. The former can be probed experimentally both by time resolved overtone pumping followed by product detection, as done by Foy, Casassa, Stephenson, and King,[4–6] or by an analysis of the overtone linewidths, as reported by Halligan.[15] The degree of internal excitation of the NH fragments can be probed by laser induced fluorescence,[4–6,11] or REMPI detection[16] and, of the N_2 fragments, by 2 + 1 REMPI detection, as reported by Dagdigian and co-workers[17] for N_2 fragments resulting from the UV photolysis of HN_3.[18–20]

The relative enthalpies for dissociation of HN_3 to $NH + N_2$ [Eqs. (1) and (2)] or to the other spin-allowed product channel

$$HN_3(\tilde{X}\,^1A') \rightarrow N_3(\tilde{X}\,^2\Pi_g) + H(^2S), \qquad (3)$$

will play an important role in determining the relative

[a] Alexander von Humboldt Senior U.S. Scientist, 1989–1990. Permanent address: Department of Chemistry, University of Maryland, College Park, Maryland 20742.

 0021-9606/90/173307-12$03.00

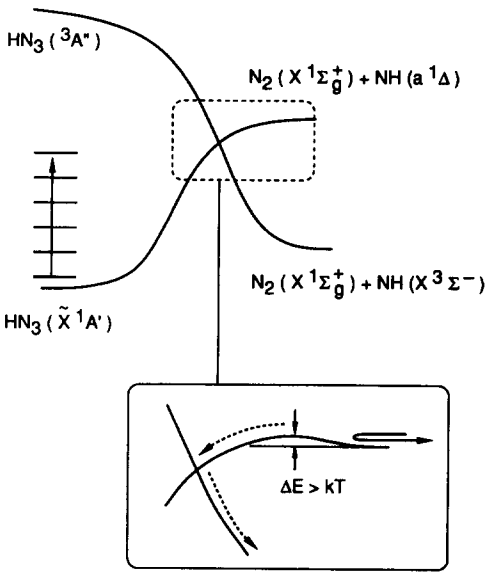

FIG. 1. Schematic reaction coordinate diagram for the energetics of the dissociation of HN_3 by vibrational overtone pumping on the ground electronic surface.

branching ratios in the UV dissociation of HN_3, as well as controlling the exothermicity of the abstraction reaction

$$H(^2S) + N_3(\tilde{X}\,^2\Pi_g) \rightarrow NH(X\,^3\Sigma^-, a^1\Delta) + N_2(X\,^1\Sigma_g^+), \quad (4)$$

now under study in Dagdigian's laboratory.[21]

In the IRMPD study of Stephenson, Casassa, and King[11] the NH fragments in the spin-allowed [$NH(a\,^1\Delta)$] channel were found to be translationally excited ($E_{tr} \approx 1700$ cm^{-1}). This implies the existence of a barrier in the exit channel, the potential energy of which is subsequently released into the translational recoil energy of the dissociating fragments. A barrier in the exit channel for dissociation could also explain the low rate constant for quenching of $NH(a\,^1\Delta)$ by N_2 ($k_q = (6\text{–}8)\times 10^{-14}$ cm^3/molecule s).[20,22,23] From the temperature dependence of the quenching rate constant the barrier was estimated to be 450 ± 40 cm^{-1}.[23] In the absence of a barrier, quenching should be efficient, mediated by approach on the singlet surface followed by crossing to the triplet surface (Fig. 1). In the isoelectronic system, $O(^1D) + N_2$, the quenching rate constant is known to be fast ($k_q = 5.5\times 10^{-11}$ cm^3/molecule s).[24] The mechanism, proposed some time ago by Fisher and Bauer,[25] involves approach on the attractive ^1N_2O potential surface followed by a spin–orbit mediated crossing to the ^3N_2O surface which then correlates to the ground state product channel, namely

$$O(^1D) + N_2 \rightarrow {}^1N_2O \rightarrow {}^3N_2O \rightarrow O(^3P) + N_2. \quad (5)$$

The goal of the present article is to characterize by *ab initio* calculations the lowest singlet and triplet surfaces of HN_3 and the lowest doublet and quartet surfaces of N_3 in the vicinity of the crossings which are relevant to the dissociation processes (1)–(4). The calculations presented here are considerably more sophisticated than those described previously.[9] Concurrently, we have obtained theoretical estimates of the dissociation enthalpies, and of the zero-point corrections to the activation energies. The details of the *ab initio* calculations are described in the next section. The discussion of the barriers to both spin-forbidden and spin-allowed dissociation is found in Sec. III. Section IV contains a discussion of the bond dissociation energies. A brief conclusion follows.

II. QUALITATIVE DESCRIPTION OF THE ORBITAL DYNAMICS ACCOMPANYING THE DECOMPOSITION OF HN_3 AND DESCRIPTION OF *AB INITIO* CALCULATIONS

In its ground ($\tilde{X}\,^1A'$) electronic state the HN_3 molecule is planar with a nearly linear N_3 moiety and the H–N bond strongly bent with respect to the N_3 backbone.[26] The wave function can be written in a single-configuration approximation as $1a'^2 \cdots 9a'^2\, 1a''^2\, 2a''^2$.[27–29] Here the $1a'$–$3a'$ molecular orbitals correspond to the inner-shell N $1s$ orbitals; the $4a'$–$9a'$ orbitals to linear combinations of the atomic s and in-plane N $2p$ orbitals, and the $1a''$ and $2a''$ orbitals to linear combinations of the out-of-plane N $2p$ orbitals. A number of *ab initio* studies of HN_3 have been reported.[9,27–31] Most have concentrated on the region of the experimental minimum, although Lievin, Breulet, and Verhaegen[31] have used SCF-CI calculations to explore the singlet $HN_3 \rightarrow N_2 + NH$ dissociation channel. Recently, Yarkony[27] has reported MCSCF-CI calculations of both the lowest singlet ($^1A'$) and triplet ($^3A''$) surfaces of HN_3, as well as the spin–orbit coupling matrix elements, in the region of the seam of crossing between these surfaces.

Qualitatively, the occurrence of barriers in both the spin-allowed and spin-forbidden decomposition of HN_3 and N_3 can be understood in terms of the energetics of the nonbonding p orbitals on the NH or N fragments. At large NN–NH distances the molecular orbitals of HN_3 become associated with either the N_2 or NH fragment, as described in Table I. In particular, in C_s geometry the degenerate $N_2\,\pi$ orbitals correlate with the $10a'$ and $2a''$ orbitals. In general, as the fragments approach, the energy of the in-plane $10a'$ orbital will increase, due to Pauli repulsion between the σ and π nonbonding orbitals on NH and the σ lone pair orbital

TABLE I. Description of HN_3 orbitals at large NN–NH distances.

Orbital	Description
$1a'$–$3a'$	$1s$ N orbital
$4a'$	σ_g orbital on N_2
$5a'$	$2s$ orbital on N of NH
$6a'$	σ_g orbital on N_2
$7a'$	σ_u orbital on N_2
$8a'$	$\pi_u(a')$ orbital on N_2
$9a'$	NH σ bonding orbital
$10a'$	$2p(a')$ orbital on N atom of NH
$11a'$	$\pi_g(a')$ orbital on N_2
$1a''$	$\pi_u(a'')$ orbital on N_2
$2a''$	$2p(a'')$ orbital on N atom of NH
$3a''$	$\pi_g(a'')$ orbital on N_2

on each of the N atoms in the N_2 molecule. Accordingly, the energy of the triplet state of HN_3, in which both the $10a'$ and $2a''$ orbitals are singly occupied and triplet coupled, increases strongly with decreasing NN–NH distance.

The lowest singlet asymptote, which corresponds to $N_2(X\,^1\Sigma_g^+) + NH(a\,^1\Delta)$, is doubly degenerate. In C_s geometry the component of this degenerate pair which is symmetric (A') with respect to reflection of the electronic spatial coordinates in the plane of the molecule corresponds to the electronic occupancy $\cdots 9a'^2 10a'^2 1a''^2 - \cdots 9a'^2 1a''^2 2a''^2$, while the component which is antisymmetric with respect to reflection (A'') corresponds to the electronic occupancy $\cdots 9a'^2 10a' 1a''^2 2a''$. This latter is the same electronic occupancy as the triplet state, except that here the singly filled orbitals are singlet coupled. Exactly as in the case of the triplet state, as the NN–NH distance decreases, the energy of the singlet state of A'' symmetry will increase. In the case of the singlet state of A' symmetry, Pauli repulsion can be minimized by orienting the NH fragment perpendicular to the N–N bond and by confining the two nonbonding NHπ orbitals to the out-of-plane $2a''$ orbital. In a simplistic analysis the bonding in HN_3 is due to the slight stabilization of this $2a''$ orbital, which is nonbonding at large NN–NH distances. The confinement of the two NH π electrons, which, asymptotically, can occupy either the π_x or π_y orbitals, to a single orbital ($2a''$) is the origin of the barrier in the exit channel of the singlet surface.

To characterize quantitatively the orbitals and energetics of the N_3 and HN_3 molecules, in particular in the region of the spin-forbidden crossings of relevance to the ground state dissociation channels, it is necessary to use an *ab initio* technique which allows for the orbital distortion and changes in electronic occupancies which accompany the breaking of the N–N bonds, which were discussed qualitatively in the preceding paragraphs of this section. This can be best done using multiconfiguration self-consistent field (MCSCF)[32–36] and multireference configuration-interaction (MCSCF-CI)[37,38] techniques. We have carried out MCSCF and complete active space self-consistent field (CASSCF)[36] calculations for the HN_3 molecule at a number of geometries. The dominant configurations from the CASSCF calculations were then selected as input into subsequent MCSCF-CI calculations. These methods are implemented in the MOLPRO-89 package of *ab initio* programs,[39] which has been used for all the calculations reported in this paper. Further, all calculations described below were restricted to coplanar geometries for HN_3.

Calculations were carried out with two different basis sets: The first consisted of, for N, Huzinaga's[40,41] $11s$, $7p$ basis with the innermost six s functions and four p functions contracted, supplemented by two d functions with exponents 1.6 and 0.4; and, for H, Huzinaga's $7s$ set with the innermost four s functions contracted supplemented by two p functions with exponents 1.2 and 0.3. This 11/7/2–7/2 basis, which is identical to the basis used in our earlier calculations[9] as well as those of Yarkony,[27] contains 94 contracted Gaussian-type orbitals. The second basis set was built on van Duijneveldt's[42] $13s$, $8p$ set for N with the first eight s and five p functions contracted and van Duijneveldt's $8s$ set for H with the first five s functions contracted. The polarization functions were taken from the recent correlation consistent triple zeta basis of Dunning,[43] and consisted of, for N, two d functions with exponents 1.654 and 0.469 and one f function with exponent 1.093, and, for H, two p functions with exponents 1.407 and 0.388 and one d function with exponent 1.057. This 13/8/2/1–8/2/1 basis contained 129 contracted Gaussian functions.

The valence space of the HN_3 molecule includes 13 orbitals and 16 electrons (excluding the $1s$ orbitals of the N atom). To keep the calculations within manageable size, in the complete active space (CASSCF) calculations for HN_3 we eliminated from the active space the highest sigma antibonding orbital, which corresponds asymptotically to the N_2 $2s_\sigma^*$ orbital—a CAS(16,12) calculation, where we have introduced the notation CAS(n,m) with n and m denoting, respectively, the number of valence electrons and the number of orbitals in the active space. In many of the calculations we also eliminated the next highest sigma antibonding orbital, which corresponds asymptotically to the NH σ^* orbital, leading to CAS(16,11) calculations. Typically these CASSCF calculations involved between several thousand and several tens of thousand configuration state functions (CSFs).

Subsequently, CI calculations were carried out, using the "internally contracted" technique of Werner and Knowles,[44,45] and including all single and double excitations out of a reference space, built from the CAS reference by including all CSFs with coefficient greater than δ in the CAS wave function. We shall designate this threshold by the notation CI(δ). In most cases this threshold was taken to by 0.04, which typically gave rise to a reference space of 10–30 CSFs. These CI(0.04) calculations involved up to a total of $\approx$750 000 contracted (12 000 000 uncontracted) configurations for the largest basis set (13/8/2/1–8/2/1). In some calculations we used a higher threshold of $\delta = 0.1$, which restricted the reference space to the dominant CSF plus those three CSFs corresponding to $\pi \rightarrow \pi^*$ excitations of the N_2 moiety, namely $\pi_x^2 \rightarrow (\pi_x^*)^2$, $\pi_y^2 \rightarrow (\pi_y^*)^2$, and the singlet coupled $\pi_x \pi_y \rightarrow \pi_x^* \pi_y^*$ excitation.

As well as shedding light on the location and topology of the barriers to dissociation, the present calculations can provide valuable theoretical input into the determination of the HN–NN and H–NNN bond dissociation energies. For this, it is important to treat electron correlation as evenhandedly as possible for both the combined and separated moieties. One problem is that the lowest dissociation asymptote $[N_2 + NH(X\,^3\Sigma^-)]$ is of higher multiplicity, and therefore has a smaller correlation energy, than the asymptote $[N_2 + NH(a\,^1\Delta)]$ which correlates with the HN_3 molecular ground state. Because of this differential correlation effect our calculated NH $a\,^1\Delta \leftarrow X\,^3\Sigma^-$ energy splitting is $\sim$600 cm^{-1} too large. To minimize the differential correlation effect in the determination of the HN–NN dissociation energy, we have calculated the energy difference for dissociation to the $N_2 + NH(a\,^1\Delta)$ asymptote. To determine the bond dissociation energy for dissociation to the $N_2 + NH(X\,^3\Sigma^-)$ asymptote, we then subtract the experimental NH $a \leftarrow X$ excitation energy, namely $T_e = 12\,664$

cm^{-1}.[10] Also, in an attempt to minimize the size consistency error, the energy of the separated fragments was determined by a supermolecule calculation, including both fragments at infinite separation, with the same basis set, valence space, and reference space selection criteria as for the calculation of the bound fragments. Subsequent to the variational MCSCF-CI calculations, the contribution of higher excitations to the total energies of the separated and combined fragments was determined by performing multireference averaged coupled pair calculations (MRACPF)[46] using identical orbitals and reference configurations as in the variational MCSCF-CI calculations. For comparison the effect of higher-order excitations was also estimated using the approach proposed by Langhoff and Davidson.[47]

Table II presents our calculated energies for HN_3 at the experimental equilibrium geometry.[26] Since our goal was not the determination of the structure and spectroscopic constants of this molecule, no geometry optimization was performed.

III. BARRIERS TO DECOMPOSITION: HN_3

Since a four atom system can be described by six internal coordinates, the locus of crossings between the $^1A'$ and $^3A''$ surfaces of the HN_3 molecule is a five-dimensional hypersurface. By restricting ourselves to planar geometries, the dimensionality is reduced by one. Our earlier, less sophisticated calculations[9] established that at the point of the minimum crossing, the terminal N–N bond distance and the N–H bond distance were very close to the experimental equilibrium internuclear separations in the ground electronic states of these two molecules [2.074 bohr for N_2 ($X\,^1\Sigma_g^+$) and 1.958 bohr for NH ($X\,^3\Sigma^-$)];[48] the interior NN–N distance was ~ 3.5 bohr; and the HN_3 geometry remained *trans* with an NNN angle slightly less than 180° and an NNH angle of nearly 90°, a value considerably larger than at the HN_3 equilibrium.[26] We subsequently carried out a series of CAS(16,11) + CI(0.1) calculations with the 11/7/2–7/2 basis to characterize further both the singlet and triplet surfaces in the region of the lowest singlet–triplet crossing. While the NN and NH bond distances were held to the values in the isolated molecules, a full variation was made of the two polar angles and the NN–NH distance. Although only planar geometries were considered, a crude estimate of the dependence of the energy on the NN–NH dihedral angle was obtained by calculations for *cis* and *trans* geometries with the same NNN and NNH polar angles.

In the region of the lowest singlet and triplet crossing the singlet and triplet surfaces were fit to a multidimensional polynomial expansion. With this fit the minimum crossing point was found to occur at a NN–NH distance of 3.35 bohr, an NNH angle of 88.7° and a *trans* NNN angle of 161°. The dependence of the energy of these surfaces on the NN–NN distance and on the NNH and NNN angles is depicted in Figs. 2 and 3. In the region of the crossing between the singlet and triplet surfaces the two diabatic wave functions will be mixed by the small spin–orbit term in the Hamiltonian. In his recent *ab initio* calculation Yarkony[27] has reported a value of 39 cm^{-1} for this matrix element, in good agreement with our previous estimate[9] of ~ 45 cm^{-1}. Significant mixing of the two states can thus occur only when the energy gap between them is $\lesssim 100$ cm^{-1}. Since (Fig. 2) the splitting between the surfaces is larger than this except right at the crossing seam, we conclude that significant nonadiabatic mixing will be confined to the region of the seam.

The saddle point on the adiabatic surface, with respect to the energy of the HN_3 $\tilde{X}\,^1A'$ ground state, will define the height of the barrier for formation of N_2 ($X\,^1\Sigma_g^+$) + NH($X\,^3\Sigma^-$) by spin-forbidden decomposition (Fig. 1). Our fit to the CAS(16,11) + CI(0.1) calculations with the 11/7/2–7/2 basis yields a barrier height of 13 830 cm^{-1} above the calculated energy of HN_3 ($\tilde{X}\,^1A'$) at the experimental equilibrium geometry (Table II). This energy difference refers to the bottom of the HN_3 well.

To obtain a more accurate value of the barrier to spin-forbidden decomposition, we have carried out a series of

TABLE II. *Ab initio* energies for the ground electronic state HN_3 ($\tilde{X}\,^1A'$) at the experimental equilibrium geometry.[a]

Basis set and method	Energy (hartree)		
	MCSCF-CI	MCSCF-CI + Q[b]	MRACPF[c]
11/7/2–7/2, MCSCF-CI[d]	− 164.203 543		
11/7/2–7/2, CAS(16,11) + CI(0.1)	− 164.431 113		
11/7/2–7/2, CAS(16,11) + CI(0.04)	− 164.441 442	− 164.490 269	
11/7/2–7/2, CAS(10,12) + CI(0.04)	− 164.446 338		
13/8/2/1–8/2/1, CAS(16,11) + CI(0.04)	− 164.491 951	− 164.547 034	− 164.538 907

[a] For HN_3: $r(N_1N_2) = 1.015$ Å, $r(N_2N_3) = 1.243$ Å, $\angle(HNN) = 108.8°$, $\angle(NNN) = 171.3°$; a planar *trans* $N_1N_2N_3H$ geometry is assumed; see Ref. 26.

[b] Contribution of higher-order excitations estimated by Davidson correction (Ref. 47).

[c] Contribution of higher-order excitations determined by multireference averaged coupled pair calculations (Ref. 46).

[d] Reference 27.

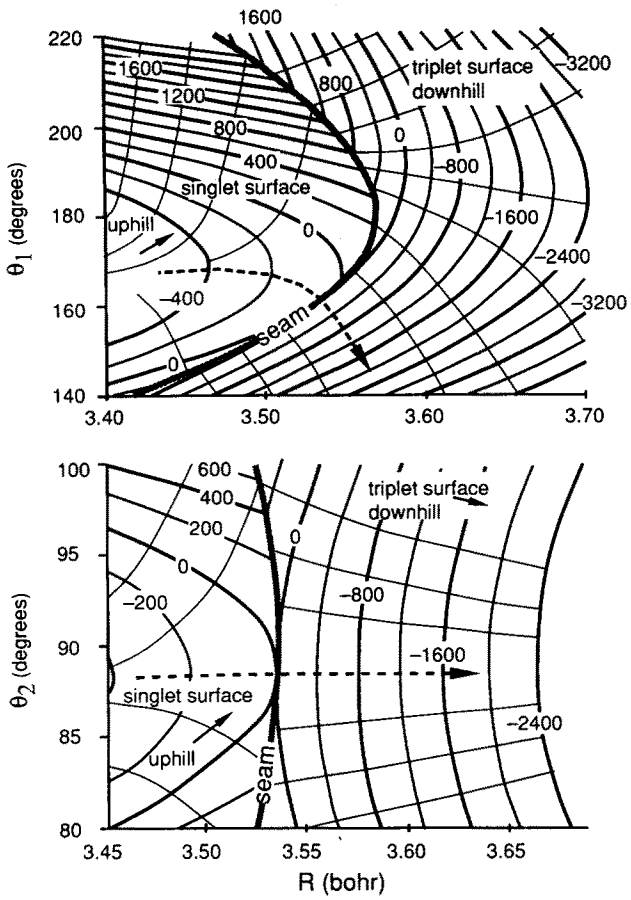

FIG. 2. Contour plot of the lowest HN_3 singlet and triplet potential energy surfaces (cm^{-1}) in the region of the minimum singlet–triplet crossing from MCSCF-CI calculations with an 11/7/2–7/2 basis (see Sec. II). The coordinates of the minimum crossing point are: $R_{N\text{-}NNH} = 2.074$ bohr, $R_{N\text{-}H} = 1.958$ bohr, $R_{NN\text{-}NH} = 3.354$ bohr, $\theta_1[\angle(NNN)] = 161.3°$, $\theta_2[\angle(HNN)] = 88.7°$. A planar geometry is assumed and the terminal NN bond is *trans* to the NH bond. The independent variables for the upper panel are R and θ_1 and, for the lower panel, R and θ_2. The zero of energy corresponds to the lowest point of crossing. In both panels the triplet surface lies to the right; the singlet surface to the left. Contours are indicated at every 400 cm^{-1} for the triplet surface and at every 200 cm^{-1} for the singlet surface. The seam which defines the locus of crossing between the two surfaces is marked. The dashed arrow indicates the minimum energy path for spin-forbidden decomposition.

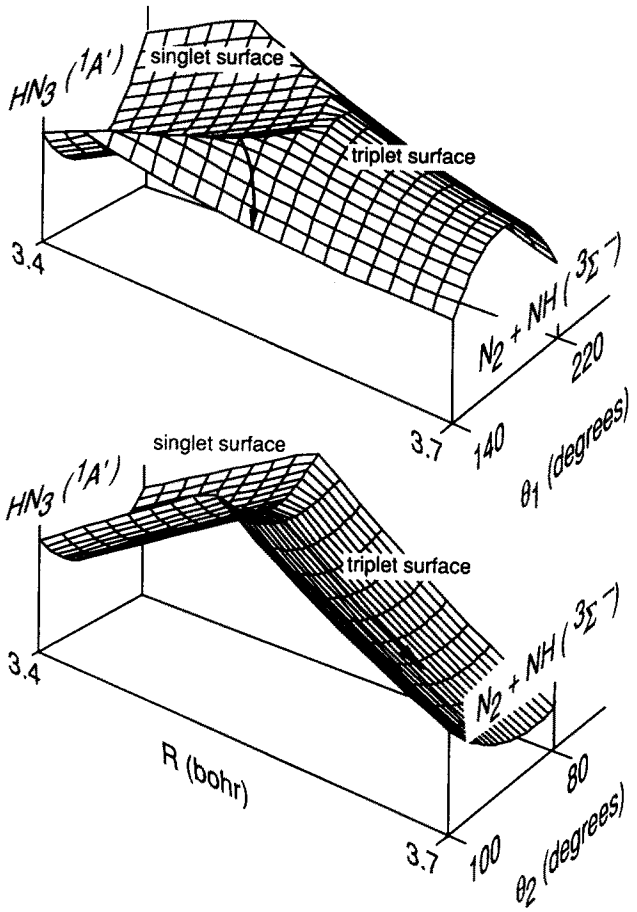

FIG. 3. Projection of the lowest HN_3 singlet and triplet potential enegy surfaces (cm^{-1}) in the region of the minimum singlet–triplet crossing from MCSCF-CI calculations with an 11/7/2–7/2 basis (see Sec. II). The coordinates of the minimum crossing point are: $R_{N\text{-}NNH} = 2.074$ bohr, $R_{N\text{-}H} = 1.958$ bohr, $R_{NN\text{-}NH} = 3.354$ bohr, $\theta_1[\angle(NNN)] = 161.3°$, $\theta_2[\angle(HNN)] = 88.7°$. A planar geometry is assumed and the terminal NN bond is *trans* to the NH bond. The independent variables for the upper panel are R and θ_1 and, for the lower panel, R and θ_2. The arrow indicates the minimum energy path for spin-forbidden decomposition. The contour plots corresonding to these two panels appear in Fig. 2.

CAS(16,11) + CI(0.04) calculations with the both the 11/7/2–7/2 and larger 13/8/2/1–8/2/1 bases (Sec. II). In these calculations the NNH and NNN angles were restricted to 90° and 165°, respectively, values close to those predicted for the minimum singlet–triplet crossing with the smaller calculations discussed in the preceding two paragraphs. Again, a planar geometry was assumed and the terminal NN and NH bond lengths were kept fixed at the equilibrium internuclear separations in the ground electronic states of N_2 and NH. Probably because these calculations allow a successively improved description of the electron correlation in the HN_3 molecule at equilibrium, relative to the more separated transition state with a correspondingly more diffuse electron distribution, the predicted barrier increases, to 14 840 cm^{-1} for the calculations with the 11/7/2–7/2 basis and to 16 230 cm^{-1} with the 13/8/2/1–8/2/1 basis. In these larger calculations the point of crossing is now found to occur at an NN–NH distance of 3.52 bohr, ~0.15 bohr larger than the value found with the smaller calculations. This can be rationalized by the fact that the singlet state is lowered relative to the triplet state, as the treatment of correlation is improved.

As discussed in Sec. II, in order to investigate the effect of higher-order excitations we also determined the singlet–triplet crossing point, still with the larger 13/8/2/1–8/2/1 orbital basis, using the MRACPF method of Gadnitz and Alrichs[46] as well as with the Davidson[47] correction. In both cases the predicted crossings are shifted hardly at all and the barrier height, relative to the calculation at equilibrium with these corrections for higher-order excitations (Table II), is increased, only slightly in the MRACPF calculations (16 330 cm^{-1}) and somewhat more with the Davidson correction (16 890 cm^{-1}).

We observe that our predicted barrier with the 11/7/2–

7/2 basis is $\sim 1100\ cm^{-1}$ *lower* than the value predicted by Yarkony.[27] Yarkony used state-averaged MCSCF orbitals[49,50] while we optimized the MCSCF orbitals separately for the $^1A'$ and $^3A''$ states. Secondly, Yarkony excluded the N 2*s* orbitals from the active space. Also, the CI procedures were not equivalent. We observe from Table II that Yarkony's calculation recovers a substantially smaller fraction of the total correlation energy of the HN_3 molecule. Despite this shortcoming, however, Yarkony's prediction for the vertical $^1A' \rightarrow {}^3A''$ excitation energy at the equilibrium geometry is 37 295 cm^{-1}, which differs insubstantially from the value of 37 284 cm^{-1} predicted by our CAS(16,11) + CI(0.04) calculation with the 11/7/2–7/2 basis.

Table III summarizes the predicted barrier heights for the spin-forbidden decomposition of HN_3. In order to compare with thermochemical estimates[12–14] of the activation energy for decomposition of HN_3 as well as those from the overtone pumping[4–6] and linewidth[15] measurements, it is necessary to correct the calculated barrier heights for the difference in zero-point energy of the HN_3 molecule at equilibrium and at the barrier.

From the known vibrational constants of HN_3,[29] which are listed in Table IV, the zero-point energy at equilibrium is calculated to be 4583 cm^{-1}. To estimate the zero-point energy at the barrier, we construct the diabatic potential energy matrix, using our polynomial fits to the singlet and triplet surfaces as the diagonal elements of this matrix and assuming a constant off-diagonal spin–orbit coupling element of 39 cm^{-1}.[27] The resulting matrix is diagonalized analytically. This expression was then used to calculate the diagonal and off-diagonal harmonic force constants for the NN–NH

TABLE IV. Vibrational frequencies (in cm^{-1}) of HN_3 at equilibrium and at the barriers to spin-forbidden and spin-allowed HN–NN decomposition.[a]

Vibration	Equilibrium[b]	Singlet–triplet crossing	Singlet saddle point
ν_1 (N–H stretch)	3497	3282[c]	3282[c]
ν_2 (N–N stretch)	2140	2358[c]	2358[c]
ν_3 (in-plane NNH wag)	1265	1067	771
ν_4 (NN–NH stretch)	1151	7721*i*	220*i*
ν_5 (in-plane NNN wag)	527	154	165
ν_6 (NN–NH torsion)	587	228[d]	139[d]

[a] In both cases a planar *trans* $N_1N_2N_3H$ geometry is assumed. At equilibrium $r(N_1N_2) = 1.9181$ bohr, $r(N_2N_3) = 2.349$ bohr, $\angle(HNN) = 108.8°$, $\angle(NNN) = 171.3°$; see Ref. 26. At the singlet–triplet crossing $r(N_1N_2) = 2.074$ bohr, $r(NH) = 1.958$ bohr, $r(N_2N_3) = 3.354$ bohr, $\angle(NNN) = 161.3°$, $\angle(HNN)] = 88.7°$; see Sec. III. At the singlet saddle point $r(N_1N_2) = 2.074$ bohr, $r(NH) = 1.958$ bohr, $r(N_2N_3) = 4.45$ bohr, $\angle(NNN) = 163°$, $\angle(HNN)] = 85°$.
[b] Reference 29.
[c] Value assumed equal to vibrational constant in isolated molecule; Ref. 48.
[d] Values for this out-of-plane motion were estimated from the difference in the energies of *cis* and *trans* planar HN_3.

TABLE III. Barrier height, activation energy, and bond dissociation energy estimates for the spin-forbidden decomposition of HN_3 [$HN_3(\tilde{X}\,^1A') \rightarrow N_2(X\,^1\Sigma_g^+) + NH(X\,^3\Sigma^-)$].[a]

Method	E_a (cm^{-1})[b]	E_0 (kJ/mol)[b]	D_0 (*kJ/mol*)[b]
11/7/2–7/2, CAS(16,11) + CI(0.1)	13 830	153	
11/7/2–7/2, CAS(16,11) + CI(0.04)	14 840	165	− 2.2
11/7/2–7/2, MCSCF-CI[c]	15 950		
13/8/2/1–8/2/1, CAS(16,11)	14 460	159	− 4.1
13/8/2/1–8/2/1, CAS(16,12)	14 870	164	11.2
13/8/2/1–8/2/1, CAS(16,11) + CI(0.04)	16 230	182	27.6
13/8/2/1–8/2/1, CAS(16,11) + ACPF(0.04)[d]	16 330	183	36.7
13/8/2/1–8/2/1, CAS(16,11) + CI(0.04) + Q[e]	16 890	189	49.9
SCF + CI[f]		~125	− 33.5
BAC-MP_4[g]			56.5
Experiment		165[h]	45 ± 6[i]
		150[j]	
		116[k]	

[a] The geometry of the minimum singlet–triplet crossing was determined by a CAS(16,11) + CI(0.1) calculation with the 11/7/2–7/2 basis.
[b] The quantity E_a designates the energy difference from the bottom of the reactant well to the transition state while E_0 is E_a with zero-point corrections added, as described in Sec. III. The quantity D_0 is the bond dissociation energy, including zero-point corrections. 1 kJ/mol = 83.67 cm^{-1}.
[c] Reference 27.
[d] Contribution of higher-order excitations determined by multireference averaged coupled pair calculations (Ref. 46).
[e] Contribution of higher-order excitations estimated by Davidson correction (Ref. 47).
[f] Reference 31.
[g] Result from Møller–Plesset fourth order calculation with the bond additivity correction of Melius and Binkley (Refs. 59–61).
[h] Reference 13.
[i] Reference 57.
[j] Reference 12.
[k] Reference 14.

stretch, the NNN in-plane wag, and the NNH in-plane wag. For the NN–NH out-of-plane torsion, we assume that the potential varies sinusoidally from a minimum in the *trans* configuration to a maximum in the *cis* configuration.

Because of the planar symmetry of the molecule, there are no off-diagonal force constants between the torsion and any of the other planar modes. For the N–NN and NH stretches, the harmonic force constants were taken to be those of the isolated NN and NH molecules.[48] Since the NH and N–NN distances were held fixed in our calculation of the potential surface near the triplet–singlet crossing, we were unable to determine the off-diagonal force constants between the N–NN and NH stretches and the other modes. The constants were consequently set equal to zero. We then constructed the inverse kinetic-energy matrix **G**,[51] corresponding to the internal coordinate system used in calculating the force constant matrix **F** determined as described above. The harmonic frequencies of the transition state are then the square roots of the solutions of the secular equation $|\mathbf{GF} - \lambda \mathbf{I}|$.[51] These are listed in Table IV. From these we estimate the zero-point energy at the singlet–triplet barrier to be 3580 cm^{-1}. Thus the calculated barrier heights in Table III must be reduced by ~ 1000 cm^{-1} to obtain the activation energy for the decomposition of HN_3.

Our estimate of the zero-point corrections to the barrier heights is subject to possible errors arising from the approximations; (1) that the NH and NN stretches at the barrier are uncoupled from the other, lower-frequency vibrations; (2) that the out-of-plane torsional motion is purely sinusoidal and can be well approximated from the two planar limits ($\phi = 0°$ and $\phi = 180°$); and (3) that the difference in zero-point energies at equilibrium and at the barrier can be accurately determined from harmonic frequencies alone without correction for anharmonicities. Also, we have assumed that the energy of HN_3 at equilibrium can be accurately represented by *ab initio* calculations at the *experimental* equilibrium geometry. Finally, we did not allow a full variation of the NNN and NNH angles in the calculations at the singlet–triplet barrier with the larger 13/8/2/1–8/2/1 basis. Here we estimate, based on our calculations with the smaller 11/7/2–7/2 basis (Fig. 2), that the angles chosen are sufficiently close to the true saddle point that the error in the calculated energy at the barrier is less than 200 cm^{-1}. To improve upon all these assumptions would have required geometry optimization at the CI level of both the $\tilde{X}\,{}^1A'$ HN_3 potential energy surface in the region of the equilibrium geometry and at the barrier, as well as of the lowest $^3A''$ surface at the barrier. This would have been beyond the scope of the computational resources available. Although it is difficult to assign a numerical uncertainty to the calculated singlet–triplet barrier height arising from the above assumptions, we believe that limits of $\pm$ 500 cm^{-1} would not be unreasonable.

The theoretical activation energies are compared with prior thermochemical estimates[12–14] in Table III. We observe that the theoretical values are considerably higher than all these experimental values, as well as the earlier theoretical estimate of Lieven *et al.*[31] from SCF-CI calculations with a much smaller basis set than used here. However, the recent overtone pumping experiments of King, Stephenson, Foy, and Casassa[5] support our theoretical estimate of the activation barrier. In these experiments HN_3 is pumped at a number of frequencies ranging from 14 400 to 17 700 cm^{-1} both on direct overtones of the NH stretch and on several intercombination bands. Both the lifetime of the excited HN_3 molecule and the vibronic state of the NH fragment are measured. When the overtone pumping frequency is increased from 15 100 to 16 229 cm^{-1}, the lifetime drops by several orders of magnitude from 210 to 5 ± 2.5 ns, but then drops by only by a factor of 2 or 3 as the frequency is further increased to 17 671 cm^{-1}.[5] The steep drop between 15 100 and 16 229 cm^{-1} suggests that the activation energy for the spin-forbidden decomposition channel lies somewhere between these limits (181–194 kJ/mol), which would be in excellent agreement with the present theoretical calculations.

The product internal energy distributions of the nascent N_2 and NH molecules produced by the singlet–triplet crossing during the $HN_3 \rightarrow N_2(X\,{}^1\Sigma_g^+) + NH(X\,{}^3\Sigma^-)$ decomposition will be sensitive to the forces exerted on the nascent products as the system crosses over from the $^1A'$ to the $^3A''$ surface. As is obvious from Figs. 2 and 3, product recoil will be virtually uncoupled from the NNH angle, so that the large energy release which occurs as the N_2–NH system falls down the triplet surfaces (Figs. 2 and 3) will not be transferred, to any significant extent, into rotational excitation of the NH fragment. This is consistent with experiment[4–6,11] as well as with the conclusions of our previous study.[9] By contrast, it is clear from Figs. 2 and 3, that product recoil *will* be coupled with the NNN angle, so that considerable rotational excitation of the N_2 products might be expected. As yet, there have been no probes of the internal energy of the N_2 fragments from the ground state decomposition of HN_3, although Dagdigian and co-workers[17] have used $2+1$ REMPI detection to probe the N_2 fragments resulting from the UV photolysis of HN_3. Interestingly enough, in the latter study a large degree of rotational excitation of the N_2 products was seen.

We turn now to a discussion of the barrier in the spin-allowed (singlet) channel in the decomposition of HN_3 (Fig. 1). By an extensive series of CAS(16,12) calculations with the 11/7/2–7/2 basis we were able to locate the saddle point in the singlet surface at an NN–NH distance of 4.45 bohr, an NNH angle of 85.0° and a *trans* NNN angle of 163°. As in our previous investigation of the barrier to spin-forbidden decomposition, we restricted our search to planar geometries and assumed that the NH and terminal NN distances were equal to the equilibrium values in the isolated molecules. Except for the larger value of the NN–NH distance, the geometry of the barrier is remarkably similar to that of the point of lowest singlet–triplet crossing. As discussed in Sec. II above, the occurrence of a barrier in the spin-allowed decomposition channel is a result of removing the $10a'$ orbital, which asymptotically correlates with one of the π orbitals on NH, from the occupied space. This qualitative prediction is supported by Fig. 4, where we plot the energies of the pseudocanonical $10a'$ and $2a''$ orbitals from CAS(16,12) calculations as a function of the NN–NH dis-

tance, holding the NNN angle equal to 170° and the NNH angle equal to 90°. We also plot the coefficient of the $\cdots 9a'^2 10a'^2 1a''^2$ and $\cdots 9a'^2 1a''^2 2a''^2$ configurations in the CASSCF wave function. Asymptotically, both orbitals become degenerate and the coefficient goes to $\sim -1/\sqrt{2}$, since the electronic occupancy of the $a\ ^1\Delta$ state of NH can be written $\pi_x^2 - \pi_y^2$. As anticipated in Sec. II, as the NN–NH distance decreases, the energy of the $10a'$ orbital increases. At the point where this orbital energy becomes positive, the weight of the $\cdots 10a'^2 1a''^2$ configuration in the CASSCF wave function dramatically decreases, since the $10a'$ orbital moves out of the filled space.

Alternatively, as we,[52] and others,[27,31] have discussed, the approach of the N_2 molecule leads to a mixing between the component of the $a\ ^1\Delta$ state of NH which has A' symmetry in C_s geometry and which is described by the asymptotic electronic occupancy $\pi_x^2 - \pi_y^2$, and the higher, nondegenerate $b\ ^1\Sigma^+$ state, which is described by the asymptotic electronic occupancy $\pi_x^2 + \pi_y^2$. With decreasing NN–NH distance the lower of these mixed states becomes increasingly described by the electronic occupancy $\pi_y^2(\cdots 9a'^2 1a''^2 2a''^2)$ and the higher, by the electronic occupancy $\pi_x^2(\cdots 9a'^2 10a'^2 1a''^2)$. As anticipated in Sec. II, the other component of the $^1\Delta$ state, which is described asymptotically by a singlet-coupled $\pi_x \pi_y$ electronic occupancy, will be purely repulsive as the NN–NH distance decreases, since the $10a'$ orbital will remain occupied, exactly as in the case of the triplet A'' state of HN_3. Figure 5 illustrates the splitting between the four states which correlate with $N_2 + NH(X\ ^3\Sigma^-, a\ ^1\Delta, b\ ^1\Sigma^+)$, as determined by CAS(16,12) calculations with the 11/7/2–7/2 basis. This system is, of course, a particular example of the general family of biradical and biradicaloid systems, which have been well studied in the organic chemical literature.[53,54]

The CAS(16,12) calculations predict the height of the barrier to spin-allowed decomposition to be $\sim 1200\ cm^{-1}$ above the $N_2 + NH(a\ ^1\Delta)$ asymptote. To obtain a more accurate value of the barrier to spin-allowed decomposition, we carried out a series of CAS(16,11), CAS(16,12), and CAS(16,11) + CI(0.04) calculations with the larger 13/8/2/1–8/2/1 basis (Sec. II). In these calculations the NNH and NNN angles were restricted to 88° and 163°, respectively, values close to those predicted for the saddle point with the smaller CASSCF calculations discussed in the preceding paragraphs. Again, a planar geometry was assumed and the terminal NN and NH bond lengths were kept fixed at the experimental equilibrium internuclear separations in the ground electronic states of N_2 and NH. The results of these calculations are given in Table V. The saddle point is now found to occur at slightly shorter NN–NH distances of ($\sim$4.2 bohr). The CASSCF, MCSCF-CI, and MRACPF[46] calculations with the larger 13/8/2/1–8/2/1 orbital basis all are in fairly close agreement in predicting a barrier height in the range of 1200–1300 cm^{-1}, relative to the $NH(a\ ^1\Delta)$ asymptote. By contrast, the Davidson correction[47] predicts a slightly *reduced* saddle point of $\sim$900 cm^{-1}.

The zero-point energy at the barrier in the spin-allowed dissociation channel can be determined by fitting the CAS(16,12) results and extracting vibrational constants. These are given in Table IV. The predicted barrier heights with zero-point corrections are also listed in Table V. Since

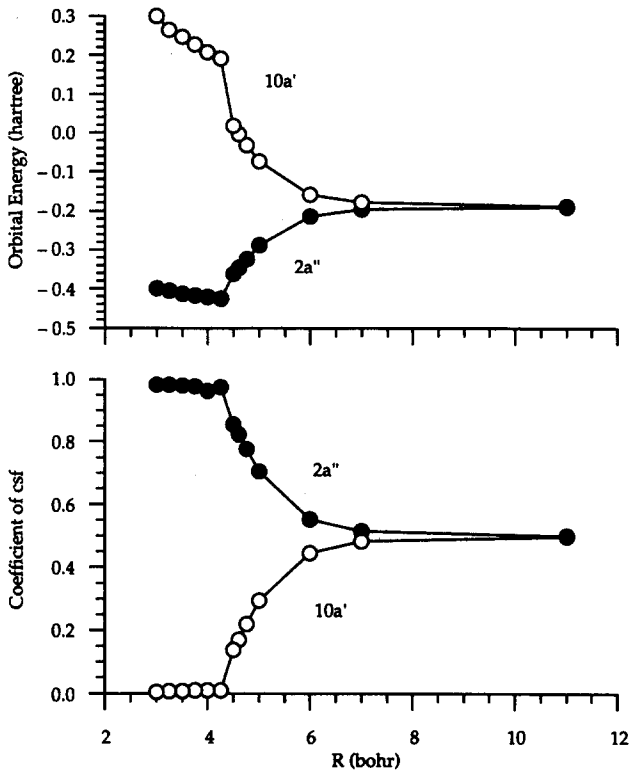

FIG. 4. (Upper panel) Energy (hartree) of the pseudocanonical $10a'$ orbital of HN_3 as a function of the NN–NH distance as given by CAS(16,12) calculations with the 11/7/2–7/2 orbital basis. For these calculations the geometry of the HN_3 molecule is *trans* planar with the NNH angle held at 90° and the NNN angle held at 170° (Lower panel) the coefficients of the $1a'^2 \cdots 9a'^2 10a'^2 1a''^2$ and $1a'^2 \cdots 9a'^2 1a''^2 2a''^2$ configurations in the CASSCF wave function for the lowest HN_3 state of $^1A_1$ symmetry. The asymptotic value of both the orbital energy and the wave function coefficients are indicated.

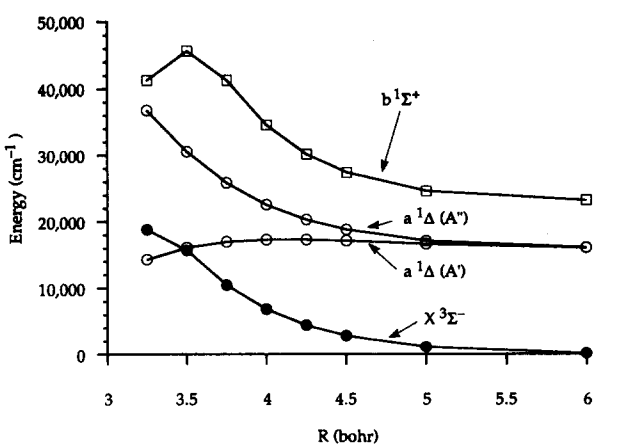

FIG. 5. Energies (cm^{-1}) of the $^3A''$, $^1A'$, and $^1A''$ states of HN_3 which correlate with the $N_2 + NH(X\ ^3\Sigma^-, a\ ^1\Delta, b\ ^1\Sigma^+)$ asymptotes, as a function of the NN–NH distance. The results refer to CAS(16,12) calculations with the 11/7/2–7/2 orbital basis. For these calculations the geometry of the HN_3 molecule is *trans* planar with the NNH angle held at 90° and the NNN angle held at 170°. Asymptotically, the A' component of the $^1\Delta$ state is described by a $\pi_x^2 - \pi_y^2$ electronic occupancy; the $^1\Sigma^+$ state, by a $\pi_x^2 + \pi_y^2$ electronic occupancy; and the A'' component of the $^1\Delta$ state as well as the $^3\Sigma^-$ state, by, respectively, singlet and triplet coupled $\pi_x \pi_y$ electronic occupancies.

the singlet barrier occurs at such an extended NN–NH distance, our assumption that the NN and NH stretches can be decoupled from the wagging modes is justified to a greater than in the case of the singlet–triplet barrier. Thus we estimate that the uncertainties in our estimate of the zero-point correction to this barrier are no larger than ± 200 cm^{-1}. Additionally we give values for the predicted activation energy, including zero-point corrections, for the spin-allowed decomposition of HN_3.

In the IRMPD study of the decomposition of HN_3,[11] using Doppler spectroscopy, Stephenson and co-workers determined the average translational energy of the NH($a\ ^1\Delta$) fragments to be ~ 1700 cm^{-1}, with an estimated uncertainty of ± 500 cm^{-1}.[55] Analysis of the vibrational overtone pumping experiments in the NIST group suggest that the barrier in the singlet channel is $\sim 1{,}200$ cm^{-1},[56] in excellent agreement with the predictions of our CASSCF, MCSCF-CI, and MRACPF calculations. As mentioned in the Introduction, the barrier in the NH($a\ ^1\Delta$) + N_2 decomposition channel can also be estimated from measurement of the activation energy for the NH($a\ ^1\Delta$) + N_2 $\rightarrow$NH($X\ ^3\Sigma^-$) + N_2 quenching reaction. However, the barrier height so obtained (450 ± 50 cm^{-1})[23] is considerably lower than both our predictions and the experimental estimate from the NIST group. The origin of this discrepancy is not yet understood.

In a recent study, Hack and Mill[22] have reported that the rate of quenching of NH($a\ ^1\Delta, v'' = 1,2$) by N_2 is virtually insensitive to the vibrational quantum number. This despite the fact that in $v'' = 2$ the energy available to the HN + N_2 system is at least 5000 cm^{-1} above the barrier on the $^1A'$ surface. Our calculations offer a simple explanation: at the barrier, the NH moiety is oriented nearly perpendicular to the NN–N chain, so that NH stretching will not be strongly coupled with the NN$\leftrightarrow$N motion which is necessary for passage over the barrier.

In the vibrational overtone pumping experiments NH($a\ ^1\Delta$) products were *not* observed after excitation to $6\nu_{NH}$ (17 670 cm^{-1})[4] but observed after excitation to $6\nu_{NH} + \nu_4$(18,755 cm^{-1}).[56] This implies that the activation energy for the spin-allowed decomposition of HN_3 into NH($a\ ^1\Delta$) + N_2, lies between 17 760 cm^{-1} and 18,755 cm^{-1}. This is consistent with the results of our MCSCF-CI and MRACPF calculations with the 13/8/2/1–8/2/1 basis set which predict (Table V) this barrier to lie between 17 000 and 17 500 cm^{-1}. One possible way to localize the height of this barrier to greater precision would be further vibrational overtone pumping experiments utilizing additional combination bands lying between $6\nu_{NH}$ and $7\nu_{NH}$.[56]

IV. HN_3 BOND DISSOCIATION ENERGIES

There is no established literature value for the heat of formation of HN_3. Estimates in the literature for the dissociation energy of the HN–NN bond in this molecule range from 46[57] to 73 kJ/mol.[13] The dissociation energy D_0 of the

TABLE V. Barrier height and activation energy for the spin-allowed decomposition of HN_3 [$HN_3(\tilde{X}\ ^1A') \rightarrow N_2(X\ ^1\Sigma_g^+) + NH(a\ ^1\Delta)$].[a]

Method	$R_{HN\text{-}NN}$ (bohr)[a]	E_a (cm^{-1})[b]	E_{0r} (cm^{-1})[b]	E_{0f} (cm^{-1})[b]
11/7/2–7/2, CAS(16,12)	4.45	1210	1740	
13/8/2/1–8/2/1, CAS(16,11)	4.24	1350	1880	14 200
13/8/2/1–8/2/1, CAS(16,12)	4.36	1170	1700	15 400
13/8/2/1–8/2/1, CAS(16,11) + CI(0.04)	4.26	1363	1901	16 900
13/8/2/1–8/2/1, CAS(16,11) + ACPF(0.04)[c]	4.25	1210	1750	17 500
13/8/2/1–8/2/1, CAS(16,11) + CI(0.04) + Q[d]	4.24	915	1450	18 300
Experiment			1740 ± 500[e]	$\geq 17\,700$[f]
			1200[g]	$\leq 18\,755$[f]
			450 ± 40[h]	

[a] The length of the NH and the terminal NN bonds, and the HNN and NNN angles at the saddle point in the exit channel, were determined by a CAS(16,12) calculation with the 11/7/2–7/2 basis. The HN–NN distance was then varied to locate the maximum in the barrier.

[b] The quantity E_a designates the energy difference from the saddle point to the product channel at infinite separation; E_{0r} is E_a with zero-point corrections added; and E_{0f} is the activation energy, including zero-point corrections, for the spin-allowed decomposition of HN_3.

[c] Contribution of higher-order excitations determined by multireference averaged coupled pair calculations (Ref. 46).

[d] Contribution of higher-order excitations estimated by Davidson correction (Ref. 47).

[e] Reference 11. Barrier height estimated from translational energy in NH($a\ ^1\Delta$) fragment in IRMPD experiments.

[f] Lower limit inferred from lack of detection of NH($a\ ^1\Delta$) products after excitation of the $v = 6$ overtone of the NH stretch (Refs. 4–6); upper limit inferred from appearance of NH($a\ ^1\Delta$) products after excitation of the $6\nu_{NH} + \nu_4$ combination band (Ref. 56).

[g] Reference 56. The tabulated value is the estimate of the total kinetic energy in NH($a\ ^1\Delta$) + N_2 products after one-photon pumping of the $v = 7$ overtone of the NH stretch.

[h] Reference 23. Barrier height estimated from temperature dependence of rate constant for quenching of NH($a\ ^1\Delta$) by N_2.

TABLE VI. Bond dissociation energy estimates for the spin-allowed decomposition of HN_3 $[HN_3(\tilde{X}\,^1A') \rightarrow N_3(\tilde{X}\,^2\Pi_g) + H(^2S)]$.

Method	D_e (cm^{-1})[a]	D_0 (kJ/mol)[a]
11/7/2–7/2, CAS(16,11) + CI(0.04)	31 112	341
13/8/2/1–8/2/1, CAS(16,11) + CI(0.04)	31 914	350
13/8/2/1–8/2/1, CAS(16,11) + CI(0.04) + Q[b]	33 289	367
BAC-MP4[c]		372
Experiment[d]		384 ± 21

[a] The quantity D_e is the dissociation energy from the minimum of the HN_3 well; the quantity D_0 is the bond dissociation energy including zero-point corrections. The zero-point energy of N_3 was taken to be 1938 cm^{-1} calculated from the gas phase value of ν_3 given by Bernath *et al.* (Ref. 65) and the matrix isolation values of ν_1 and ν_2 given by R. Tian, J. C. Facelli, and J. Michl, J. Phys. Chem. **92**, 4073 (1988).

[b] Contribution of higher-order excitations estimated by Davidson correction (Ref. 47).

[c] Result from Møller–Plesset fourth order calculation with the bond additivity correction of Melius and Binkley (Refs. 59–61).

[d] Reference 58.

$H–N_3$ bond has been estimated by Pellerite *et al.* to be 3.99 ± 0.22 eV (384 ± 21 kJ/mol).[58]

Melius and Binkley have determined heats of formation for a number of polyatomics by adding a bond additivity correction (BAC) to the results of fourth order Møller–Plesset (MP4) perturbation theory calculations of the molecular energies.[59–61] The basis sets used in these MP4 calculations were much smaller than those used here. Using the BAC-MP4 heats of formation of HN_3, NH, N, and H,[59–61] we predict dissociation energy of 56.5 and 372 kJ/mol for the HN–NN and H–NNN bonds, respectively.

We have calculated dissociation energies for the HN–NN and H–NNN bonds in HN_3 using the technique discussed in Sec. II. The values are compared with available experimental estimates and the BAC-MP4 predictions of Melius and Binkley[59–61] in Tables III and VI.

For fission of the $H–N_3$ single bond (Table VI), the calculated dissociation energies change hardly at all when the 11/7/2–7/2 orbital basis is replaced by the larger 13/8/2/1–8/2 basis, which indicates most likely that even the smaller basis provides an adequate description of the differential correlation effects associated with fission of this bond. The calculated values, especially when corrections for higher-order excitations are included, are in excellent agreement with both the experimental estimate[58] and the prediction of Melius and Binkley.[59–61]

For the multiple NN–NH bond the calculated dissociation energy (Table III) is very sensitive to the inclusion of f functions on the N atoms. Indeed, the MCSCF + CI calculations with the 11/7/2–7/2 basis predict a negative dissociation energy. The MCSCF + CI calculation with the larger 13/8/2/1–8/2/1 basis predicts a positive dissociation energy (27.6 kJ/mol). With the corrections for higher-order excitations included in the MRACPF calculations,[46] which will lower the energy of the HN_3 molecule slightly with respect to the energy of the fragments, the calculated dissociation energy (36.7 kJ/mol) is higher, but still somewhat less than the lower (46 ± 5 kJ/mol[57]) of the experimental estimates for this quantity. However, the present theoretical estimates are considerably lower than the BAC-MP4 prediction of Melius and Binkley.[59–61]

V. CONCLUSIONS

This article has been devoted to an *ab initio* investigation of the energetics of the spin-allowed and spin-forbidden decomposition of HN_3. By means of MCSCF + CI calculations with large orbital basis sets, we have obtained reliable estimates of the location and heights of the barriers to decomposition, as well as the dissociation energy of the $N_2–NH$ bond. The predicted barrier in the lowest energy, spin-forbidden decomposition channel, $E_a = \sim 16\,500$ cm^{-1}, is larger than anticipated by earlier experimental work,[12–14] but completely consistent with the results of the recent vibrational overtone pumping experiments of King, Stephenson, Casassa, and Foy.[4–6]

The shape of the calculated triplet potential energy surface in the exit channel of the spin-forbidden decomposition channel implies that there will be little rotational excitation of the $NH(X\,^3\Sigma^-)$ fragments, consistent with the experimental results.[4,6,11] By contrast, we predict a significant torque on the departing N_2 fragment, which should manifest itself in a relatively high degree of rotational excitation. There is some experimental evidence for a substantial degree of N_2 rotational distribution in the spin-allowed $[NH(a\,^1\Delta) + N_2]$ decomposition channel.[56] We strongly encourage future experimental studies of the degree of rotational excitation of the N_2 fragment following both spin-allowed and spin-forbidden decomposition.

We also find a barrier to decomposition in the lowest spin-allowed decomposition channel of ~ 1200 cm^{-1} in height. This barrier occurs outside the spin-forbidden crossing, at an NN–NH distance of ~ 4.2 bohr. The predicted height of this barrier is consistent with the estimate obtained from the product translational energy analysis in both the IRMPD[11] and overtone pumping[56] studies of the decomposition of HN_3. It is not understood, however, why the estimate of the barrier height deduced from the temperature dependence of the quenching of $NH(a\,^1\Delta)$ by N_2 (450 ± 50 cm^{-1})[23] is substantially lower than both the present theoretical predictions and the experimental estimates of the NIST group.[11,56]

The calculated dissociation energy of the $H–N_3$ bond

($D_0 = 350$–370 kJ/mol) agrees well with both the empirically corrected *ab initio* estimate of Melius and Binkley[59–61] (372 kJ/mol) as well as the experimental value of Brauman and co-workers[58] (384 ± 21 kJ/mol). Our calculated values of the dissociation energy of the N_2–NH bond ($D_0 = 28$–37 kJ/mol) show more variation but lie close to Okabe's estimate of the dissociation energy (45 ± 6 kJ/mol), somewhat lower than the estimate of Melius and Binkley[59–61] (56.5 kJ/mol), and significantly lower than other experimental estimates.[13]

To determine these thermochemical parameters, in particular the dissociation energy of the HN–NN bond, to a higher degree of precision would certainly require the addition to the atomic orbital basis of a second *f* function on N and a *g* function. Unfortunately, this would render the resulting MCSCF-CI calculations prohibitively expensive. Given, however, the present state of experimental uncertainty, we believe that the present calculations can certainly help to delimit the range of possible values for these quantities.

We attributed the origin of the barrier in the spin-allowed decomposition of HN_3 to an effect of orbital constriction: as the N_2–NH distance decreases Pauli repulsion with the lone-pair σ orbital on the N_2 forces one of the NH π orbitals out of the occupied space. This implies, then, that in N_2–AB systems with one less (or one more) π electron on the AB molecule, as for example N_2–CH($X\,^2\Pi$) or N_2–OH($X\,^2\Pi$) there will be no barrier as the N_2–AB distance is decreased. Interestingly enough, in reported *ab initio* calculations[62] on the NNCH system, Bair and Dunning find no evidence of a barrier as the NN–CH bond is broken.

Similar barriers to both spin-allowed and spin-forbidden decomposition will certainly occur in related systems, such as N_3, NCO, and HNCO. In the latter case, no barrier is expected in the singlet channel [NH($a\,^1\Delta$) + CO($X\,^1\Sigma^+$)], since the rate constant for quenching of NH($a\,^1\Delta$) by CO is large and shows no evidence of an activation energy.[20,23] *Ab initio* calculations on several of these systems are in progress, and will be reported shortly.

The present article is limited to the description of the lowest singlet and triplet potential surfaces of the HN_3 molecule in those regions of space of greatest importance for the lowest energy decomposition processes. Hopefully this description will subsequently be useful in simulating the dynamics of the decomposition process itself, in particular the variation in the lifetime of the excited HN_3 molecules as a function of the overtone excitation wavelength, which has been measured in such detail by the NIST group.[4–6] Simple RRKM theory predicts decomposition rates which are many orders of magnitude larger than observed.[5] Likely this is a consequence of the spin-forbidden nature of the decomposition process. As discussed by Yarkony,[27] a simple Landau–Zener treatment predicts that at energies above the singlet–triplet crossing, but below the barrier to the spin-allowed channel, the probability associated with singlet–triplet transitions will be very small. More accurate, but still simple, treatments can be developed,[63] which provide an essentially exact description of spin-forbidden decomposition down into the tunneling region, as well as at higher energies where both the spin-allowed and spin-forbidden channels are open.

Note added in proof: In related work, U. Meier and V. Staemmler (to be published) have explored both planar and non planar geometries relevant to the UV photolysis of HN_3.

ACKNOWLEDGMENTS

The research described here was partially supported by the U.S. Air Force Office of Scientific Research under Contract No. F49620-88-C-0056. The calculations were carried out on the CRAY XMP48 at the San Diego Supercomputer Center, under an allocation of time to MHA in connection with NSF Grant No. CHE87-05828, and on the CRAY YMP832 at the Höchstleistungsrechenzentrum der Kernforschungsanlage Jülich, Federal Republic of Germany, under a grant of time to M.H.A. and H.J.W. The participation of H.J.W. was made possible by the Deutsche Forschungsgemeinschaft and by the German Fonds der Chemischen Industrie. M.H.A. is grateful to David King and Michael Casassa for unpublished information about their experimental studies; to David Yarkony for discussions about the calculations presented here; to Carl Melius for the results of some unpublished BAC-MP4 heats of formation (Ref. 61), to Thom Dunning for information about the studies of the CH + N_2 potential surface reported in Ref. 62, and to Walter Hack for a preprint of Ref. 64.

[1] For a good review, see *Molecular Photodissociation Dynamics*, edited by J. Baggott and M. N. R. Ashfold (Royal Society of Chemistry, London, 1987).
[2] For a recent review, see J. P. Simons, J. Phys. Chem. **91**, 5378 (1987).
[3] R. Bersohn, J. Phys. Chem. **88**, 5145 (1984).
[4] B. R. Foy, M. P. Casassa, J. C. Stephenson, and D. S. King, J. Chem. Phys. **89**, 608 (1988).
[5] B. R. Foy, M. P. Casassa, J. C. Stephenson, and D. S. King, J. Chem. Phys. **92**, 2782 (1990).
[6] B. R. Foy, M. P. Casassa, J. C. Stephenson, and D. S. King, J. Chem. Phys. **90**, 7037 (1989).
[7] X. Luo, P. T. Rieger, D. S. Perry, and T. R. Rizzo, J. Chem. Phys. **89**, 4448 (1988).
[8] F. F. Crim, in *Molecular Photodissociation Dynamics*, edited by M. N. R. Ashfold and J. E. Baggott (Royal Society of Chemistry, London, 1987), and references contained therein.
[9] M. H. Alexander, H.-J. Werner, and P. J. Dagdigian, J. Chem. Phys. **89**, 1388 (1988).
[10] The experimental excitation energy of NH, $T_0(a \leftarrow X)$, is 12 688.39 cm^{-1} [C. R. Brazier, R. S. Ram, and P. F. Bernath (BRB), J. Mol. Spectrosc. **120**, 381 (1986)]. We estimate the value of the rotationless T_e to be 12 664 cm^{-1}. This is obtained by adding to T_0 the difference in the zero-point energies in the $a\,^1\Delta$ and $X\,^3\Sigma^-$ states, which we estimated using values of ω_e and $\omega_e x_e$ calculated from the vibrational term values given in Tables IX and X of BRB (see footnote e to Table III of Ref. 9), and then subtracting the rotational energy of the lowest ($J = 2$) state of NH($a\,^1\Delta$).
[11] J. C. Stephenson, M. P. Casassa, and D. S. King, J. Chem. Phys. **89**, 1378 (1988).
[12] O. Kajimoto, T. Yamamoto, and T. Fueno, J. Phys. Chem. **83**, 429 (1979).
[13] C. Paillard, G. Dupré, and J. Combourieu, J. Chim. Phys. **82**, 489 (1985).
[14] A. I. Demin, I. S. Zaslonko, S. M. Kogarko, and E. V. Mossuhkin, Kinet. Katal. **14**, 283 (1973) (in Russian, as cited in Ref. 13).
[15] M. Halligan, Ph.D. thesis, Rice University, 1988.
[16] K.-H. Gericke, R. Theinl, and F. J. Comes, Chem. Phys. Lett. **164**, 605 (1989).
[17] J.-J. Chu, P. Marcus, and P. J. Dagdigian, J. Chem. Phys. **93**, 257 (1990).
[18] A. P. Baronavski, R. G. Miller, and J. R. McDonald, Chem. Phys. **30**, 119 (1978).
[19] L. G. Piper, R. H. Krech, and R. L. Taylor, J. Chem. Phys. **73**, 791 (1980).
[20] F. Freitag, F. Rohrer, and F. Stuhl, J. Phys. Chem. **93**, 3170 (1989).
[21] J. Chen, E. Quiñones, and P. J. Dagdigian, J. Chem. Phys. **93**, 257 (1990).

[22] W. Hack and A. Wilms, J. Phys. Chem. **93**, 3540 (1989).
[23] H. H. Nelson, J. R. McDonald, and M. H. Alexander, J. Phys. Chem. (to be published).
[24] T. G. Slanger and G. Black, J. Chem. Phys. **60**, 468 (1974).
[25] R. Fisher and E. Bauer, J. Chem. Phys. **57**, 1966 (1972).
[26] B. P. Winnewiser, J. Mol. Spectrosc. **82**, 220 (1980).
[27] D. R. Yarkony, J. Chem. Phys. **92**, 320 (1990).
[28] S. W. Harrison, C. R. Fischer, and P. J. Kemmey, Chem. Phys. Lett. **36**, 229 (1975).
[29] C. E. Sjögren and C. E. Nielsen, J. Mol. Struct. **142**, 285 (1986).
[30] D. J. deFrees, G. H. Loew, and A. D. McLean, Astrophys. J. **254**, 405 (1982).
[31] J. Lievin, J. Breulet, and G. Verhaegen, Theor. Chim. Acta **52**, 75 (1979).
[32] H.-J. Werner and W. Meyer, J. Chem. Phys. **73**, 2342 (1980), and references contained therein.
[33] H.-J. Werner, Adv. Chem. Phys. **49**, 1 (1987), and references contained therein.
[34] H.-J. Werner and W. Meyer, J. Chem. Phys. **74**, 5794 (1981).
[35] H.-J. Werner and P. J. Knowles, J. Chem. Phys. **82**, 5053 (1985).
[36] P. J. Knowles and H.-J. Werner, Chem. Phys. Lett. **115**, 259 (1985).
[37] H.-J. Werner and E. A. Reinsch, in *Advanced Theories and Computational Approaches to the Electronic Structure of Molecules*, edited by C. E. Dykstra (Reidel, Dordrecht 1984), p. 79.
[38] H.-J. Werner and P. J. Knowles, J. Chem. Phys. **89**, 5803 (1988).
[39] MOLPRO is a package of *ab initio* programs written by H.-J. Werner and P. J. Knowles, with contributions from J. Almlöf, R. Amos, S. Elbert, W. Meyer, E. A. Reinsch, R. Pitzer, and A. Stone.
[40] S. Huzinaga, J. Chem. Phys. **42**, 1293 (1965).
[41] S. Huzinaga, Department of Chemistry, University of Alberta, Canada, 1965.
[42] F. B. van Duijneveldt, IBM Res. Rep. RJ 945 (1971).
[43] T. H. Dunning, J. Chem. Phys. **90**, 1007 (1989).
[44] P. K. Knowles and H.-J. Werner, Chem. Phys. Lett. **145**, 514 (1988).
[45] H.-J. Werner and P. J. Knowles, J. Chem. Phys. **89**, 5803 (1988).
[46] R. J. Gadnitz and R. Alrichs, Chem. Phys. Lett. **143**, 413 (1988).
[47] S. R. Langhoff and E. R. Davidson, Int. J. Quantum Chem. **8**, 61 (1974).
[48] K. P. Huber and G. Herzberg, *Molecular Spectra and Molecular Structure. IV. Constants of Diatomic Molecules* (Van Nostrand Reinhold, New York, 1979).
[49] B. H. Lengsfield, J. Chem. Phys. **77**, 4073 (1982).
[50] R. N. Diffenderfer and D. R. Yarkony, J. Phys. Chem. **86**, 5098 (1982).
[51] E. B. Wilson, J. C. Decius, and P. C. Cross, *Molecular Vibrations* (McGraw-Hill, New York, 1955).
[52] M. H. Alexander, H.-J. Werner, and P. J. Dagdigian, J. Chem. Phys. **89**, 1388 (1988).
[53] L. Salem, *Electrons in Chemical Reactions* (Wiley, New York, 1982).
[54] V. Bonacic-Koutecky, J. Koutecky, and J. Michl, Angew. Chem. Int. Ed. Engl. **26**, 170 (1987).
[55] J. C. Stephenson and D. S. King (private communication, 1988).
[56] D. S. King, B. R. Foy, and M. P. Casassa (to be published).
[57] H. Okabe, *Photochemistry of Small Molecules* (Wiley, New York, 1978).
[58] M. J. Pellerite, R. L. Jackson, and J. I. Brauman, J. Phys. Chem. **85**, 1624 (1981).
[59] C. F. Melius and S. Binkley, in *21st Symposium (Intl) on Combustion* (The Combustion Institute, Pittsburgh, 1986), p. 1953.
[60] P. Ho, M. E. Coltrin, J. S. Binkley, and C. F. Melius, J. Am. Chem. Soc. **89**, 4647 (1985).
[61] C. F. Melius and S. Binkley, in *20th Symposium (Intl) on Combustion* (The Combustion Institute, Pittsburgh, 1984), p. 575.
[62] R. A. Bair and T. H. Dunning, Annual Report, Theoretical Chemistry Group Chemistry Division, Argonne National Laboratory (1985).
[63] M. H. Alexander, G. Parlant, and T. Hemmer, J. Chem. Phys. **91**, 2388 (1989).
[64] W. Hack and T. Mill (to be published).
[65] C. R. Brazier, P. F. Bernath, J. B. Burkholder, and C. J. Howard, J. Chem. Phys. **89**, 1762 (1988).